**RAA 2019** Vol. **19** No. **10**, 153(7pp) doi: 10.1088/1674–4527/19/10/153

*http://www.raa-journal.org* *http://iopscience.iop.org/raa*

***R**esearch in*
***A**stronomy and*
***A**strophysics*

# On the weak Ly$\alpha$ emission line of BL Lacertae objects

Jia Bu[1,2], Ren-Yi Ma[1,2], Tao-Tao Fang[1,2], Xiao-Di Yu[1,2] and Xin-Wu Cao[2,3]

[1] Department of Astronomy and Institute of Theoretical Physics and Astrophysics, Xiamen University, Xiamen 361005, China; *ryma@xmu.edu.cn, fangt@xmu.edu.cn*

[2] SHAO-XMU Joint Center for Astrophysics, Xiamen 361005, China

[3] Shanghai Astronomical Observatory, Chinese Academy of Sciences, Shanghai 200030, China

Received 2019 April 5; accepted 2019 May 21

**Abstract** Recent studies reveal that weak Ly$\alpha$ emission line may be a ubiquitous feature of nearby BL Laceratae objects (BL Lacs). We present a survey of the Ly$\alpha$ emission lines in BL Lacs, with a focus on data obtained by the Cosmic Origins Spectrograph onboard the *Hubble Space Telescope*. Among the 11 selected targets, seven show a clear detection of the intrinsic Ly$\alpha$ emission line, while one manifests a marginal detection. Two of these intrinsic Ly$\alpha$ lines are newly detected in this work (FBQS J1217+3007 and 3C 66A). Most selected BL Lacs are either high or intermediate-frequency peaked BL Lacs, with the only exception being one low-frequency peaked BL Lac. A strong anti-correlation between the line equivalent width and the continuum luminosity was found. The possible sources of ionizing photons that are responsible for production of the Ly$\alpha$ emission line are studied based on a widely accepted detailed accretion-jet model. It is found that the clouds of the broad line region are unlikely to be located in the jet cone region with an inclination angle of less than 10 degrees. Contributions from the jet and disk to the emission lines are found to be comparable. Additionally, a possible way to constrain the accretion rate from the emission line is proposed.

**Key words:** galaxies: active — BL Lacertae objects: general — ultraviolet: galaxies — galaxies: jets

## 1 INTRODUCTION

A blazar is a type of active galactic nucleus (AGN) with a relativistic jet beaming towards us (e.g., Blandford & Rees 1978; Urry & Padovani 1995). It can be divided into two subclasses: BL Lacertae objects (or BL Lacs) and flat spectrum radio quasars (FSRQs). Unlike FSRQs, BL Lacs are intrinsically weak radio sources with little or no emission features. The lack of emission lines that is typically seen in many other AGNs is attributed to the overwhelmingly strong, beamed emission from the jet. The broadband spectral energy distribution (SED) of BL Lacs can be characterized by synchrotron emission from the relativistic jet, which typically peaks in the infrared (low-frequency peaked BL Lacs, or LBLs) or in the ultraviolet (UV) and X-ray (high-frequency peaked BL Lacs, or HBLs) (see, e.g., Stickel et al. 1993; Padovani & Giommi 1995; Corbett et al. 2000). The exact reason for the differences between LBLs and HBLs is still unclear: it can be due to selection effect, viewing angles, the so-called blazar sequence or a combination of various effects (see, e.g., Perlman & Stocke 1993; Ghisellini et al. 1998; Rector & Stocke 2001; Ghisellini & Tavecchio 2008; Stocke et al. 2011).

In the past, very high signal-to-noise ratio (S/N) spectroscopy of LBLs has shown weak optical emission lines (see, e.g., Corbett et al. 2000; Rector & Stocke 2001). Recently, using UV spectrometers onboard the *Hubble Space Telescope* (*HST*), several observations revealed weak Ly$\alpha$ emission lines (Stocke et al. 2011; Fang et al. 2014; Danforth et al. 2016). These Ly$\alpha$ emission lines exhibit a typical luminosity of a few times $10^{40}\ \mathrm{erg\,s^{-1}}$. It also appears that such emission lines may be a ubiquitous feature of HBLs (Stocke et al. 2011; Danforth et al. 2016).

These weak Ly$\alpha$ emission lines in BL Lacs are in general believed to be produced in broad line regions (BLRs) around the central engine; however, the exact ionization mechanism is still unclear. Stocke et al. (2011) argued that the BLRs were ionized by isotropic ionizing flux from the jet of BL Lacs, and the difference between the predicted

and observed Ly$\alpha$ line flux can be attributed to the Doppler boost effect of the jet. However, if a hot accretion flow exists around the central engine of BL Lacs (Yuan & Narayan 2014), then it is natural to suggest that radiation from the accretion flow may also contribute to the ionizing flux (see, e.g., Foschini 2012).

For some low-luminosity AGNs (LLAGNs), due to the decrease of the mass accretion rate and hence the mass outflow rate (Yuan et al. 2012, 2015), Elitzur & Ho (2009) suggested that the BLR disappears when the accretion disk is radiatively inefficient and its luminosity is below a critical value (also see Foschini 2012)

$$L \approx 5 \times 10^{39} \left(\frac{M_{\rm BH}}{10^7\,M_\odot}\right)^{2/3} \ {\rm erg\,s^{-1}}, \qquad (1)$$

where $M_{\rm BH}$ is the mass of the central black hole. Since typically these BL Lac objects have a central black hole mass of $10^8 - 10^9\,M_\odot$, their critical luminosity is around $10^{40} - 10^{41}\,{\rm erg\,s^{-1}}$. These values are comparable with the observed Ly$\alpha$ line luminosity in our sample (see below). Because the disk luminosity will be at least an order of magnitude higher than the line luminosity to generate such line emission (Foschini 2012), the disk luminosity of the blazar must be higher than the critical value. Moreover, the disk luminosity is at least about $10^{-4}$ of the Eddington luminosity, which is high enough to play an important role in producing ionizing photons.

In this paper, we analyze the UV spectra of a sample of selected BL Lacs, focusing on their Ly$\alpha$ emission lines, and investigate the origin of the ionizing photons. Our motivation is to address an important question – Are the ionizing photons produced by the jet emission, the putative accretion disk, or a combination of both?

This paper is organized as follows. In Section 2, we describe our sample selection and measurement of the Ly$\alpha$ emission lines. In Sections 3 and 4, we analyze the jet and accretion disk as the source of the ionizing photons, respectively. Our conclusions and discussion are presented in the last section.

## 2 SAMPLE SELECTION AND THE LY$\alpha$ EMISSION LINE

Our BL Lac sample was acquired from the HST Spectroscopic Legacy Archive (HSLA)[1]. Some of these targets were discussed before with available intrinsic Ly$\alpha$ measurements (see, e.g., Stocke et al. 2011; Fang et al. 2014; Danforth et al. 2016). Most of these BL Lac objects were observed with the Cosmic Origins Spectrograph (COS) onboard *HST*, except that Mkn 501 and PKS 2155-304 were observed with the Faint Object Spectrograph (FOS) and Space Telescope Imaging Spectrograph (STIS) on *HST*, respectively.

Most BL Lac objects were observed with only the far UV (FUV) channel of COS, with a wavelength coverage of 1150−1800 Å. So, we have restricted our search to BL Lac objects at $z \lesssim 0.5$ for the Ly$\alpha$ emission line. We also focused on the BL Lac spectra with high S/N ratio. In the end, a total of 11 targets was selected. Eight of the targets exhibit a clear detection of the intrinsic Ly$\alpha$ emission line (see Table 1), among which two were newly detected in this work. Based on Nieppola et al. (2006), BL Lacs can be categorized as HBLs ($\nu_{\rm peak} \approx 10^{17-18}$ Hz), LBLs ($\nu_{\rm peak} \approx 10^{13-14}$ Hz) and the intermediate-frequency peaked BL Lacs or IBLs ($\nu_{\rm peak} \approx 10^{15-16}$ Hz). Most of our targets are either HBLs or IBLs/HBLs, with the only exception being one LBL, S5 0716+714. For the non-detections in our sample, we have estimated a $4\sigma$ upper limit of the Ly$\alpha$ luminosity and equivalent width (EW), following equation (1) in Stocke et al. (2011).

Seven targets were analyzed before by Stocke et al. (2011), Fang et al. (2014) and Danforth et al. (2016), so we adopted the measured Ly$\alpha$ parameters (or upper limits) here. Additionally, we also find two new detections, FBQS J1217+3007 and 3C 66A, implementing the method used in Fang et al. (2014). It is found that the Galactic reddening has negligible impact on the intrinsic Ly$\alpha$ emission line, thus we decided not to include this in our study. Figure 1 presents Ly$\alpha$ emission from FBQS J1217+3007 (left panel) and 3C 66A (right panel), in which the red dashed lines are Gaussian fits to the emission lines. We also present the Ly$\alpha$ emission feature in Table 2.

Since we do not know the redshift of both BL Lacs, we took an initial guess for the redshifts by visually identifying the emission features in the broadband spectra of both BL Lacs. More accurate redshifts were determined later by the line-fitting procedure. For FBQS J1217+3007, to accurately determine the Ly$\alpha$ emission line profile, we first redshifted the spectrum into the rest frame of the BL Lac and fitted the broadband continuum with a power law, $F_\lambda = F_{912}(\lambda/912\,{\rm \AA})^{-\alpha_\lambda}$. To smooth the continuum, we manually identified all the regions with strong emission/absorption features and excluded those regions in our fit. We found a power-law index of $\alpha_\lambda = 0.13 \pm 0.014$ and a normalization of $F_{912} = (1.03 \pm 0.04) \times 10^{-14}{\rm erg\,cm^{-2}\,s^{-1}}$. We then extracted the continuum and fitted the emission line with a Gaussian model. Due to the deviation of a single power-law fit to the broadband continuum at long wavelengths, we limited the fit

[1] See *https://archive.stsci.edu/hst/spectral_legacy/.*

**Table 1** Target List

| Target | RA (deg) | DEC (deg) | Type | $\log \nu_{\rm peak}$ (Hz) | $z_{\rm AGN}$ | EW (mÅ) | $I_{\rm Ly\alpha}$ ($10^{40}\,{\rm erg\,s^{-1}}$) | Reference |
|---|---|---|---|---|---|---|---|---|
| H 2356-309 | 12.84 | –78.04 | HBL | $17.87^b$ | $0.165^d$ | $1030 \pm 220$ | $9.53 \pm 2.02$ | [2] |
| PKS 2155-304 | 17.73 | –52.25 | HBL/IBL | $15.67^b$ | $0.116^d$ | $< 44$ | $< 11$ | [1] |
| 1ES 1553+113 | 21.91 | 43.96 | HBL | $16.49^a$ | $0.410^d$ | $< 76$ | $< 3.06$ | [4] |
| Mkn 501 | 63.60 | 38.86 | HBL | $16.84^a$ | $0.034^d$ | $830 \pm 83$ | $5.2 \pm 0.3$ | [1] |
| 3C 66A | 140.14 | –16.77 | IBL | $15.63^a$ | $0.339^e$ | $350 \pm 218$ | $57.6 \pm 35.9$ | [4] |
| S5 0716+714 | 143.98 | 28.02 | LBL | $14.46^a$ | $0.300^d$ | $< 61$ | $< 28.0$ | [4] |
| 1ES 1028+511 | 161.44 | 54.44 | HBL | $18.56^a$ | $0.360^d$ | $98 \pm 29^c$ | $5.8 \pm 1.7$ | [3] |
| Mkn 421 | 179.83 | 65.03 | HBL | $18.49^a$ | $0.031^d$ | $76 \pm 7$ | $2.37 \pm 0.22$ | [1] |
| FBQS J1217+3007 | 188.87 | 82.05 | IBL | $15.58^a$ | $0.130^d$ | $1404 \pm 121$ | $52.9 \pm 4.6$ | [4] |
| PMN J1103-2329 | 273.19 | 33.08 | HBL | $18.10^b$ | $0.186^d$ | $346 \pm 28^c$ | $4.9 \pm 0.4$ | [3] |
| PKS 2005-489 | 350.37 | –32.60 | HBL/IBL | $15.95^b$ | $0.071^d$ | $467 \pm 47$ | $24.9 \pm 1.1$ | [1] |

*a*: Adopted from Nieppola et al. (2006); *b*: Referenced from Fan et al. (2016); *c*: Estimated using the line flux and continuum; *d*: Acquired from the NED; *e*: Applied from this work; 1: Stocke et al. (2011); 2: Fang et al. (2014); 3: Danforth et al. (2016); 4: This work.

to the range of $1210-1225$ Å (in the rest frame of the BL Lac). We ascertained that a single Gaussian profile fits the emission line very well (see the left panel of Fig. 1). The line central wavelength in the observer's frame is $\lambda_{\rm obs} = 1374.34 \pm 0.63$ Å, corresponding to the velocity center $39129.26 \pm 156.24\,{\rm km\,s^{-1}}$. We also found that, at the $7.69\sigma$ significance level, the full width at half maximum (FWHM) is $9.17 \pm 0.94$ Å, and the EW is EW$= -1.40 \pm 0.12$ Å. We also derived a Ly$\alpha$ line flux of $(1.51 \pm 0.13) \times 10^{-14}\,{\rm erg\,cm^{-2}\,s^{-1}}$ and a luminosity of $(52.9 \pm 4.6) \times 10^{40}\,{\rm erg\,s^{-1}}$.

For 3C 66A, we followed the same procedure mentioned above and fitted the continuum in the rest frame of the BL Lac. Due to the presence of some obvious absorption features, the data around 1615 Å, 1621 Å and 1623 Å are removed during the fitting of the continuum. The fitting results are $\alpha_\lambda = 0.34 \pm 0.03$ and $F_{912} = (6.24 \pm 0.03) \times 10^{-15}{\rm erg\,cm^{-2}\,s^{-1}}$. We then fitted the emission line with a Gaussian model (see the right panel of Fig. 1). The line is weak with a significance of $\sim 2.17\sigma$, and all the relevant information is listed in Table 2.

Due to the featureless optical continuum of BL Lac objects, it is often difficult to directly measure their redshifts, and such information can only be determined by studying the spectral features or images of their host galaxies. The redshifts of most of our sample targets were robustly determined using this method; however, for two targets, 3C 66A and 1ES 1553+113, we were unable to do so. Therefore, their redshifts have to be determined or estimated using another method.

For 3C 66A, we have successfully detected the Ly$\alpha$ emission line. Based on our line-fitting procedure, we have measured a redshift of $z = 0.3398 \pm 0.0002$. This agrees extremely well with the recent result by Torres-Zafra et al. (2018), in which the redshift was identified to be 0.34 by resolving the galaxy group that hosts this blazar. By comparing GeV and TeV spectra and assuming the change in slopes is caused by the interaction between GeV photons and extragalactic background light (EBL), Prandini et al. (2010) derived an upper limit for the redshift range of $0.265-0.446$. This result is consistent with what we find here.

For 1ES 1553+113, since no intrinsic Ly$\alpha$ emission line was detected, we cannot utilize the emission line to measure the source redshift. From the lack of intergalactic Ly$\alpha$ absorption lines in its UV spectrum, Nicastro et al. (2018) derived a lower limit for the redshift of 1ES 1553+113 at $z \sim 0.41$. We adopt this value in Table 1. Using $\gamma$-ray observation of EBL absorption, Abramowski et al. (2015) estimated a redshift of $\sim 0.49 \pm 0.04$. Given the limit of redshift, we can find a $4\sigma$ upper limit of the Ly$\alpha$ luminosity with equation (1) in Stocke et al. (2011). A careful examination of the UV spectrum of 1ES 1553+113 indicates that the continuum remains almost constant from 1700 Å all the way to the end of the spectrum at 1800 Å which covers a redshift range of $0.4-0.5$ for the Ly$\alpha$ line. So, our estimated upper limit of the Ly$\alpha$ emission line would remain unchanged as long as its redshift is below $\sim 0.5$.

Furthermore, as depicted in Figure 2, we have identified a strong anti-correlation between the line EW of the Ly$\alpha$ emission line and the continuum luminosity at the redshifted wavelength of the Ly$\alpha$ line, similar to the Baldwin effect discovered in other types of AGNs (Baldwin 1977; Netzer 1985; Pogge & Peterson 1992). We fit the power-law continuum in the form $F_\lambda = F_{912}(\lambda/912{\rm Å})^{-\alpha_\lambda}$ for all our samples, and obtain the values of $F_{912}$ and $\alpha_\lambda$. So, we can determine the continuum luminosity at the redshifted

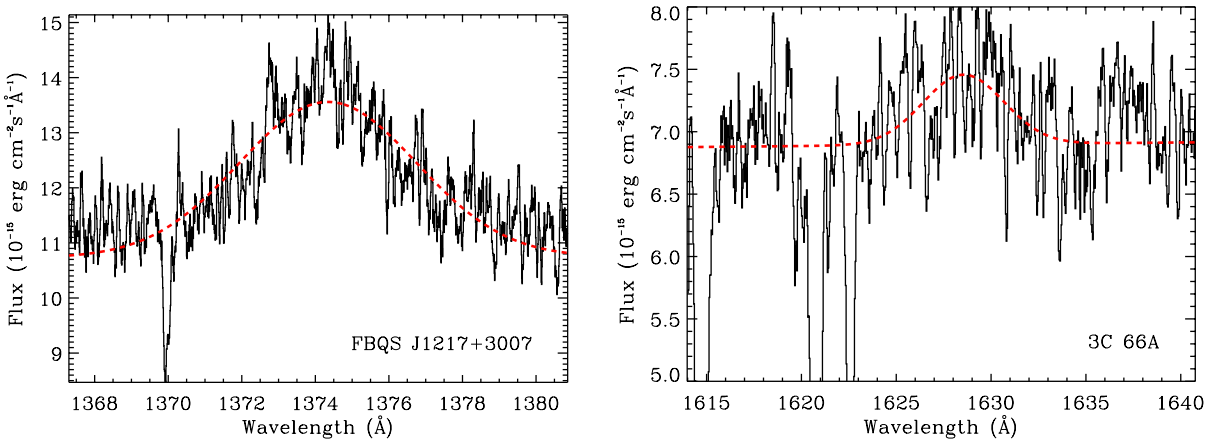


**Fig. 1** Ly$\alpha$ emission from FBQS J1217+3007 (*left panel*) and 3C 66A (*right panel*). The *red dashed lines* are Gaussian fits to the emission lines (*Color version is online*).

**Table 2** Ly$\alpha$ Emission Feature

| | FBQS J1217+3007 | 3C 66A | Unit |
|---|---|---|---|
| Centroid | $1374.34 \pm 0.63$ | $1628.04 \pm 0.25$ | Å |
| | $39129.26 \pm 156.24$ | $101813.77 \pm 64.19$ | $\mathrm{km\,s^{-1}}$ |
| FWHM | $9.17 \pm 0.94$ | $7.13 \pm 5.11$ | Å |
| EW | $-1.40 \pm 0.12$ | $-0.35 \pm 0.22$ | Å |
| Significance level | 7.69 | 2.17 | $\sigma$ |
| $I$(Ly$\alpha$) | $15.1 \pm 1.3$ | $2.41 \pm 1.50$ | $10^{-15}\,\mathrm{erg\,cm^{-2}\,s^{-1}}$ |
| $L$(Ly$\alpha$) | $52.9 \pm 4.6$ | $57.6 \pm 35.9$ | $10^{40}\,\mathrm{erg\,s^{-1}}$ |

wavelength of the Ly$\alpha$ line. Then we fit the linear relationship between the EW of the Ly$\alpha$ emission line and the continuum luminosity at the redshifted wavelength of the Ly$\alpha$ line. The linear relationship between the two quantities can be described as

$$\mathrm{EW(m\AA)} = 9 \times 10^{31} (L_{1216\mathrm{\AA}})^{-0.7}. \quad (2)$$

We have calculated the Spearman's rank order correlation coefficient, $r_s = -0.6$, suggesting a rather strong anti-correlation between these two quantities.

## 3 EMISSION FROM THE JET

We first investigate the possibility in which jet emission is the only source of ionizing photons for producing the observed Ly$\alpha$ emission line. This has been extensively discussed in Stocke et al. (2011) and Fang et al. (2014). In their works, an over-prediction factor is included to reconcile the difference between the observed Ly$\alpha$ flux and the predicted line flux from the observed continuum. However, there is no physical explanation for this factor.

There are two key assumptions in previous works. On one hand, the jet emission is assumed to be isotropic, which is obviously problematic because the bulk Lorentz factor of the jet is large and the beaming effect is significant. On the other hand, the continuum of the jet is assumed to be a simple power-law form. This should be acceptable for HBLs since the power law extends to the X-ray band, but for LBLs, or even IBLs, the continuum will be highly over-estimated.

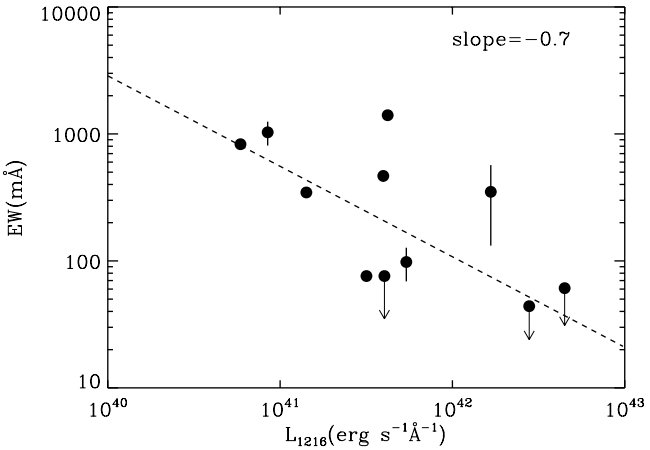


**Fig. 2** The anti-correlation between EW of the Ly$\alpha$ emission line and continuum luminosity at the wavelength of the redshifted Ly$\alpha$ emission. The slope of the fitted curve is $-0.7$.

To improve the theoretical calculation, a more detailed jet model is included in this paper. We follow the jet model described in Yuan et al. (2005) and calculate the jet emission as a function of the viewing angle. In this model, some fraction of the accreting gas is transferred into the

vertical direction and forms the jet. In the jet, shells with different velocity catch up with each other and collide, forming internal shocks. The shock can heat plasma in the jet, generate or amplify the magnetic field, and accelerate a small fraction of electrons into relativistic energy that follows the power-law energy distribution with index $p$. We collected the broadband continuum data from the NASA/IPAC Extragalactic Database (NED), along with the UV data from *HST* observations, so that the model parameters could be constrained with the multi-band SED.

Based on this model, we can now calculate the jet emission spectrum at different viewing angles $\theta$ of the BLR clouds. The jet emission is maximal at the smallest viewing angle, and minimal at the perpendicular direction. We provide an example of Mkn 421 jet emission at different viewing angles in Figure 3. The top solid line represents the broadband spectrum at the viewing angle $\theta = 2^\circ$ (viewing along the sightline toward us), and the lower solid line signifies an extreme case of the jet emission when viewing in the perpendicular direction, or $\theta = 90^\circ$. An order of five to ten magnitude difference between the two viewing angles definitely demonstrates that the isotropic emission adopted in previous works is not a good assumption.

In Table 3, for most targets, the viewing angle $\theta$ and the bulk Lorentz factor $\Gamma_j$ are adopted from Celotti & Ghisellini (2008). For 1217+3007, the values of $\theta$ and $\Gamma_j$ are referenced from Ghisellini et al. (2010). For 1ES 1028+511, we can obtain the Doppler factor $\delta$ from Fan et al. (2014), derive the upper limit of $\theta$ according to the formula $\theta_{\rm max} = \arcsin(1/\delta)$ and derive the lower limit of $\Gamma_j$ with the formula $\Gamma_{j\,\rm min} = \frac{1}{2}(\delta + 1/\delta)$. The other input parameters for this model are fixed at their typical values (see Yuan et al. 2005 for details). The only two adjustable parameters are the mass-loss rate in the jet $\dot{m}_j$ and the power-law index $p$ (Table 3).

We then follow a similar procedure to what was presented in Stocke et al. (2011) and Fang et al. (2014) to calculate the expected Ly$\alpha$ emission line flux, assuming the BLR region is optically thick. We refer readers to the above two papers for details. Instead of using an over-prediction factor, we can find the exact viewing angles $\theta_0$ of the BLR clouds (relative to the jet) by matching the calculated Ly$\alpha$ flux with the observed one. We list our results for $\theta_0$ in Table 3. Our calculations imply that to match the observed Ly$\alpha$ flux, the viewing angles for all our samples must be located in a very narrow range between $\sim 10^\circ - 15^\circ$. In fact, this value of $\theta_0$ indicates a boundary for the BLR clouds. In the range of $0^\circ < \theta < \theta_0$, if such clouds exist, the flux of the emission line would be much higher than the observed line flux due to the beaming effects. So, the BLR clouds can only be located in the range $\theta_0 < \theta < 90^\circ$. The idea that the BLR clouds lie away from the jet axis is easy to understand, because the kinetic energy of the jet can blow away the cold gas on the way, and strong emission from the jet can easily fully ionize the ambient gas. The theoretical model of Pancoast et al. (2012) and Pancoast et al. (2018) supports the case that the BLR clouds (relative to the jet) may be distributed in the range of viewing angle $\sim 0^\circ - 90^\circ$ non-uniformly. However, our results further show that the BLR clouds cannot be distributed around the jet cone, i.e., inside $\sim 10^\circ - 15^\circ$.

It is necessary to check the influence of the model parameters upon the value of $\theta_0$. We choose Mkn 421 to demonstrate such influence. The bulk Lorentz factor of the jet $\Gamma_j$ has been constrained by observations and numerical simulations (Celotti et al. 1997; Yuan et al. 2005; Gallo et al. 2003; Celotti & Ghisellini 2008; Ghisellini et al. 2010), and the range of typical values of $\Gamma_j$ for a blazar is found to be about $10-20$. When changing $\Gamma_j$ by $\pm 50\%$ (e.g., $\pm 10$), we find the change of $\theta_0$ is $\leq 1^\circ$. The mass-loss rate in the jet $\dot{m}_j$ is about 1% of the accretion rate in the accretion disk (Yuan & Cui 2005; Yuan et al. 2005; Nemmen et al. 2014), being about $10^{-5} - 10^{-8}$ in Eddington unit. When we change $\dot{m}_j$ by one order of magnitude, the change of $\theta_0$ is $\simeq \pm 4^\circ$. The power-law index $p$ is usually around 2, or in the range of $1.6-2.5$ (Yuan et al. 2005; Kirk et al. 2000). When we change $p$ by $\pm 5\%$ (e.g., $\pm 0.1$), the change of $\theta_0$ is $\leq 1^\circ$. All of these calculations above demonstrate that the value of $\theta_0$ is not very sensitive to the change of the other model parameters.

## 4 EMISSION FROM THE ACCRETION DISK

Another possible origin of the ionizing photons is the accretion disk. Compared to the jet, emission from the accretion flow is isotropic, which means all of the clouds could contribute to Ly$\alpha$ flux. Since many more clouds are included, the contribution of the accretion flow could be comparable to that of jet.

We have adopted the accretion disk model of Yuan et al. (2005) to calculate emission from the disk. This accretion-jet model consists of two components: an inner hot accretion flow and a jet. The jet model is what we used in the previous section. For the purpose of comparison, we ignore the jet here, assuming that all of the line emissions are due to the illumination of the accretion flow. By globally solving the basic differential equations of the accretion flow, we can obtain the dynamics of the flow and calculate the total spectrum, including the synchrotron, bremsstrahlung and Comptonization processes.

**Table 3** Modeling

| Target | Jet | | | | | Accretion Disk |
|---|---|---|---|---|---|---|
| | $\theta^a$ (degree) | ${\Gamma_j}^a$ | $\dot{m}_j$ ($\dot{m}_{\rm Edd}$) | $p$ | $\theta_0$ (degree) | $\dot{m}$ ($10^{-5}\dot{m}_{\rm Edd}$) |
| Mkn 421 | 2 | 18 | $1\times10^{-7}$ | 2.3 | 12 | 4.5 |
| Mkn 501 | 3 | 14 | $4\times10^{-8}$ | 2.1 | 13 | 2.6 |
| PKS 2005–489 | 2.6 | 18 | $1.3\times10^{-7}$ | 2.05 | 10.5 | 5.5 |
| PKS 2155–304 | 1.7 | 20 | $1.3\times10^{-7}$ | 2.19 | $>11.5$ | $<6.0$ |
| H 2356–309 | 2.6 | 18 | $1.2\times10^{-7}$ | 2.1 | 10.5 | 6.2 |
| 1ES 1028+511 | 1.8 | 20 | $5\times10^{-7}$ | 2.1 | 13 | 8.6 |
| PMN J1103–2329 | 1.7 | 20 | $3\times10^{-8}$ | 2.01 | 9.7 | 3.0 |
| FBQS J1217+3007 | 3 | 15 | $2.5\times10^{-6}$ | 2.05 | 10.9 | 39 |
| 3C 66A | 3 | 16 | $3.6\times10^{-6}$ | 2.1 | 13.9 | 17 |
| 1ES 1553+113 | 1.8 | 20 | $9\times10^{-7}$ | 2.1 | $>17$ | $<4.5$ |
| S5 0716+714 | 2.6 | 17 | $5\times10^{-6}$ | 2.06 | $>15.5$ | $<11.5$ |

$a$: For most sources, the viewing angle $\theta$ and the bulk Lorentz factor $\Gamma_j$ are adopted from Celotti & Ghisellini (2008). For 1217+3007, the values of $\theta$ and $\Gamma_j$ are referenced from Ghisellini et al. (2010). For 1ES1028+511, the Doppler factor $\delta$ was obtained from Fan et al. (2014). The upper limit of $\theta$ can be derived according to the formula $\theta_{\rm max}=\arcsin(1/\delta)$ and the lower limit of $\Gamma_j$ can be calculated according to the formula $\Gamma_{j\,\rm min}=\frac{1}{2}(\delta+1/\delta)$.

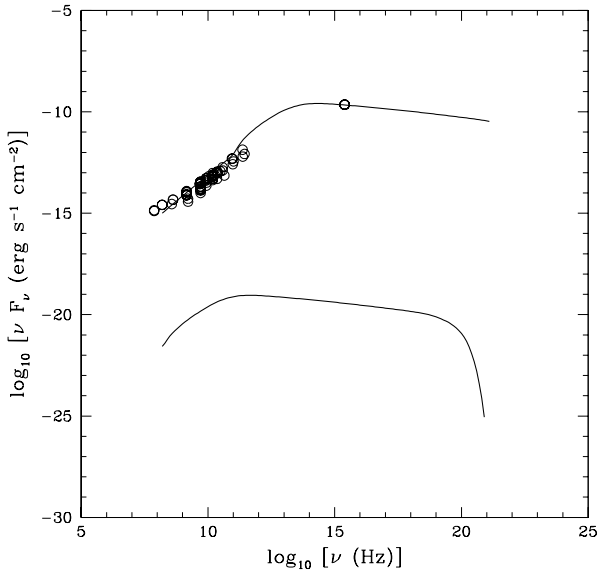


**Fig. 3** Multi-waveband fitting of the jet spectrum of Mkn 421. The radio data were adopted from NED, and the UV data from the *HST* observations. The *top* and *bottom lines* show the emission spectra of the jet with viewing angles of $2^\circ$ and $90^\circ$, respectively.

We fixed all of the model parameters at their typical values (e.g., Yuan et al. 2005) except the accretion rate at the outer boundary of the accretion flow, $\dot{m}$. The disk spectra are calculated for different accretion rats. Following the same method as described in Section 3, the expected Ly$\alpha$ emission line flux can be calculated. Consequently, the accretion rate needed to explain the observed line flux is calculated and listed in the last column of Table 3.

For a self-consistent accretion-jet model, the mass loss rate in the jet is much less than the accretion rate, which is usually less than 1% (e.g., Yuan & Narayan 2014). Comparing the values of $\dot{m}_j$ and $\dot{m}$, it could be found that their ratio is about $1-0.1\%$, which agrees with a self-consistent accretion-jet model. Inversely speaking, for a real black hole accretion system, the contribution of the jet and the hot accretion flow are comparable.

Consequently, the most likely scenario is that the accretion disk and the jet contribute ionizing photons together. It is interesting to further explore this result. Since the jet may contribute a fraction of the line flux, our calculated values of the accretion rates represent the upper limits of accretion rates for all our samples. In other words, the Ly$\alpha$ emission line may provide us a possible way to limit the accretion rate of supermassive black hole systems. It should be noted that in our calculations, the covering factor of the BLR is assumed to be 1. If the covering factor is smaller, the upper limit of the accretion rate would be higher.

## 5 SUMMARY AND DISCUSSION

In this paper, we present our analysis of the intrinsic Ly$\alpha$ emission lines of 11 BL Lacs. We summarize our findings here:

- In the 11 targets, eight show a clear detection of the intrinsic Ly$\alpha$ emission line, among which two were newly detected in this work (FBQS J1217+3007 and 3C 66A).
- We also have found a strong correlation between the line EW of the Ly$\alpha$ emission line and the continuum luminosity at the redshifted wavelength of the Ly$\alpha$ line, similar to the Baldwin effect discovered in other types of AGNs.
- Assuming the ionizing photons only come from jet emission, we have computed the expected Ly$\alpha$ emission line flux and find the exact viewing angles of

the BLR clouds (relative to the jet) by matching the calculated Ly$\alpha$ flux with the observed one. We find $\theta_0 \sim$ 10° – 15°. Considering the jet beaming effects and the real distribution of BLR clouds, our results imply that the BLR clouds must be distributed outside the jet cone region, i.e., $\theta_0 < \theta < 90°$.

– Assuming the accretion disk provides all the ionizing photons, we have also computed the expected Ly$\alpha$ emission line flux and find the accretion rates by matching the calculated Ly$\alpha$ flux with the observed one. The accretion rates we obtained are about one thousand times the mass loss rate in the jet. Since $\dot{m}_j/\dot{m} \sim 0.1\%$ is a reasonable value for an accretion-jet system, this result indicates the contributions of accretion flow and jet to the ionizing photons are comparable.
– We have also accurately determined the redshift of one of the BL Lac objects, 3C 66A. Previous observations were unable to identify its host galaxy, therefore we cannot determine the redshift. Our Ly$\alpha$ emission line measurement suggested a redshift of $z = 0.3398 \pm 0.0002$. Such method may become an effective way to measure the redshifts of these typically "featureless" BL Lac objects.

S5 0716+714 is the only LBL that also does not have a detection. It is possible that the Ly$\alpha$ emission line is present but is hidden by the strong non-thermal continuum. This provides an interesting question regarding whether or not the ubiquitous presence of the weak Ly$\alpha$ emission line only applies to the HBLs. Due to our limited sample size, we cannot draw any solid conclusion at this moment. Consequently, more observations are necessary to resolve this problem.

**Acknowledgements** We thank Drs. Feng Yuan, Jin Zhang and Tinggui Wang for helpful discussions. We also thank Dr. Yuan for providing the codes to calculate the broadband emission from the jet and accretion. This work is supported by the National Key R&D Program of China (2017YFA0402600) and the National Natural Science Foundation of China (Grant Nos. 11525312 and U1531130).

## References

Abramowski, A., Aharonian, F., Ait Benkhali, F., et al. 2015, ApJ, 802, 65
Baldwin, J. A. 1977, ApJ, 214, 679
Blandford, R. D., & Rees, M. J. 1978, Phys. Scr, 17, 265
Celotti, A., & Ghisellini, G. 2008, MNRAS, 385, 283
Celotti, A., Padovani, P., & Ghisellini, G. 1997, MNRAS, 286, 415
Corbett, E. A., Robinson, A., Axon, D. J., & Hough, J. H. 2000, MNRAS, 311, 485
Danforth, C. W., Stocke, J. T., France, K., Begelman, M. C., & Perlman, E. 2016, ApJ, 832, 76
Elitzur, M., & Ho, L. C. 2009, ApJ, 701, L91
Fan, J.-H., Bastieri, D., Yang, J.-H., et al. 2014, RAA (Research in Astronomy and Astrophysics), 14, 1135
Fan, J. H., Yang, J. H., Liu, Y., et al. 2016, ApJS, 226, 20
Fang, T., Danforth, C. W., Buote, D. A., et al. 2014, ApJ, 795, 57
Foschini, L. 2012, RAA (Research in Astronomy and Astrophysics), 12, 359
Gallo, E., Fender, R. P., & Pooley, G. G. 2003, MNRAS, 344, 60
Ghisellini, G., Celotti, A., Fossati, G., Maraschi, L., & Comastri, A. 1998, MNRAS, 301, 451
Ghisellini, G., & Tavecchio, F. 2008, MNRAS, 387, 1669
Ghisellini, G., Tavecchio, F., Foschini, L., et al. 2010, MNRAS, 402, 497
Kirk, J. G., Guthmann, A. W., Gallant, Y. A., & Achterberg, A. 2000, ApJ, 542, 235
Nemmen, R. S., Storchi-Bergmann, T., & Eracleous, M. 2014, MNRAS, 438, 2804
Netzer, H. 1985, MNRAS, 216, 63
Nicastro, F., Kaastra, J., Krongold, Y., et al. 2018, Nature, 558, 406
Nieppola, E., Tornikoski, M., & Valtaoja, E. 2006, A&A, 445, 441
Padovani, P., & Giommi, P. 1995, ApJ, 444, 567
Pancoast, A., Brewer, B. J., Treu, T., et al. 2012, ApJ, 754, 49
Pancoast, A., Barth, A. J., Horne, K., et al. 2018, ApJ, 856, 108
Perlman, E. S., & Stocke, J. T. 1993, ApJ, 406, 430
Pogge, R. W., & Peterson, B. M. 1992, AJ, 103, 1084
Prandini, E., Bonnoli, G., Maraschi, L., Mariotti, M., & Tavecchio, F. 2010, MNRAS, 405, L76
Rector, T. A., & Stocke, J. T. 2001, AJ, 122, 565
Stickel, M., Fried, J. W., & Kuehr, H. 1993, A&AS, 98, 393
Stocke, J. T., Danforth, C. W., & Perlman, E. S. 2011, ApJ, 732, 113
Torres-Zafra, J., Cellone, S. A., Buzzoni, A., Andruchow, I., & Portilla, J. G. 2018, MNRAS, 474, 3162
Urry, C. M., & Padovani, P. 1995, PASP, 107, 803
Yuan, F., Bu, D., & Wu, M. 2012, ApJ, 761, 130
Yuan, F., & Cui, W. 2005, ApJ, 629, 408
Yuan, F., Cui, W., & Narayan, R. 2005, ApJ, 620, 905
Yuan, F., Gan, Z., Narayan, R., et al. 2015, ApJ, 804, 101
Yuan, F., & Narayan, R. 2014, ARA&A, 52, 529